Heterogeneous Oxidation of Carbonyl Sulfide on Atmospheric Particles and Alumina

HONG HE,* JUNFENG LIU, YUJING MU, YUNBO YU, AND MEIXUE CHEN

State Key Laboratory of Environmental Chemistry and Ecotoxicology, Research Center for Eco-Environmental Sciences, Chinese Academy of Sciences, Beijing, 100085, China

Heterogeneous oxidation of carbonyl sulfide (OCS) on atmospheric particles and alumina (Al_2O_3) was investigated in a closed system and a flowed system using in situ diffuse reflectance infrared Fourier transform spectroscopy (DRIFTS). At room temperature, OCS could be catalytically oxidized on the surface of atmospheric particles and Al_2O_3 to form gas-phase CO_2 and surface sulfate (SO_4^{2-}), sulfite (HSO_3^-), and hydrogen carbonate (HCO_3^-) species. The real atmospheric particles were characterized using X-ray fluorescence (XRF) and the Brunauer−Emmett−Teller (BET) method. As a simplified model, Al_2O_3 was used to study the reaction mechanism of heterogeneous oxidation of OCS. The hydrogen thiocarbonate surface ($HSCO_2^-$) species, an intermediate formed in the reaction of OCS with surface hydroxyl (OH), could only be observed on the prereduced Al_2O_3 sample. The experimental results also indicate that surface oxygen containing species on the atmospheric particle sample and the Al_2O_3 sample might be the key reactant for OCS oxidation. A reaction mechanism of heterogeneous oxidation of OCS on Al_2O_3 surface is discussed.

1. Introduction

Carbonyl sulfide (OCS) is the most abundant atmospheric sulfur gas in the remote troposphere, with an average global mixing ratio of about 500 ± 50 pptv (parts per trillion by volume) (*1*, *2*). It is relatively inert in the troposphere and its tropospheric lifetime is greater than 1 year (*1*−*3*). OCS can be transported into the stratosphere where its photooxidation is considered to be an important source of stratospheric sulfate during volcanically quiescent periods (*3*−*5*). Understanding of the global OCS cycle is therefore of considerable importance partially because, so far, the known sources of OCS are not balanced with its sinks (*6*).

Most studies focus on the homogeneous reaction of OCS with OH in the gas phase and the consumption of OCS by plants, soil, etc (*6*). Heterogeneous interactions between gaseous molecules with wet or dry atmospheric particle surfaces have gained considerable interest since they have the potential to significantly alter the process of atmospheric chemistry (*3*, *7*). The surface of oxide particles in the atmosphere can adsorb and catalyze reactions of trace gases, and thus change the chemical balance of the atmosphere (*8*, *9*). However, very few studies have examined the possibility of heterogeneous reaction and the conversion pathway of

OCS on the surface of atmospheric particles. This might be due to the difficulty in studies on the heterogeneous reaction and its mechanisms of trace gases on the complex atmospheric particles.

To understand the mechanism of heterogeneous reaction of OCS on the surface of atmospheric particles, diffuse reflectance infrared Fourier transform spectroscopy (DRIFTS) was used in this study. DRIFTS can be used to obtain the nature of gas−solid surface interactions. In situ DRIFTS is especially useful to explore mechanisms of heterogeneous reaction on solid surfaces by providing information on reactive intermediates formed on the surface. Aluminum is one of the most abundant elements in atmospheric particles. It has been reported that alumina (Al_2O_3) surface catalyzes the oxidation of either H_2S or CS_2, and its catalytic property is influenced by pretreatments (*10*−*12*). Therefore, it is necessary to investigate the heterogeneous reaction of OCS on the atmospheric particles and study the reaction mechanism on the surface of alumina as a model.

In this experiment, we found that atmospheric particles and Al_2O_3 catalyze the heterogeneous oxidation of OCS at room temperature to form gas-phase CO_2 and surface sulfate (SO_4^{2-}), sulfite (HSO_3^-), and hydrogen carbonate (HCO_3^-) species, and we propose a composite reaction mechanism based on the experimental results.

2. Experimental Section

2.1. Materials. The atmospheric particle sample (21 g) was collected on the roof of an office building at the Research Center for Eco-Environmental Sciences, Chinese Academy of Science, Beijing. The Al_2O_3 sample used in this experiment was supplied by Shandong Aluminum Corporation. Before the DRIFTS measurement, the Al_2O_3 sample was pretreated in an in situ infrared cell following one of two basic procedures: the preoxidized Al_2O_3 sample obtained by heating in 100 mL/min O_2 at 573 K for 2 h; or the prereduced Al_2O_3 sample obtained by heating in 100 mL/min H_2 at 573 K for 2 h. The preoxidized atmospheric particle sample was pretreated by heating in 100 mL/min O_2 at 373 K for 2 h.

The specifications of gases used in this experiment are as follows without further purification: OCS (2%, OCS/N_2, Scott Specialty Gases Inc.), O_2 (99.99% purity, Beijing AP BEIFEN Gases Inc.), H_2 (99.999% purity, GCD-300B high purity hydrogen generator, China Bchp Analytical Technology Co. Ltd.).

2.2. Techniques of Characterization. *X-ray Fluorescence.* Inorganic elementary analysis was carried out on an Elementary Vario El (Germany) system. X-ray fluorescence (XRF) data were obtained from a Bruker S4 Explorer spectrometer.

BET Experiment. The nitrogen adsorption−desorption isotherms were obtained at 77 K over the whole range of relative pressures, using a Micromeritics ASAP 2000 automatic equipment. Specific areas were computed from these isotherms by applying the Brunauer−Emmett−Teller (BET) method.

In situ DRIFTS Experiment. In situ DRIFTS spectra were recorded on a Nexus 670 (Thermo Nicolet Instrument Corporation) FT-IR, equipped with an in situ diffuse reflection chamber and a high-sensitivity MCT detector cooled by liquid N_2. The sample for the in situ DRIFTS studies was finely ground and placed into a ceramic crucible in the in situ chamber. Mass flow controllers and a sample temperature controller were used to control the reaction conditions. The reference spectrum was measured after the pretreated sample was cooled to 298 K in a purified O_2 or H_2 stream. The infrared

* Corresponding author phone: +86-10-62849123; fax: +86-10-62849123; e-mail: honghe@mail.rcees.ac.cn.
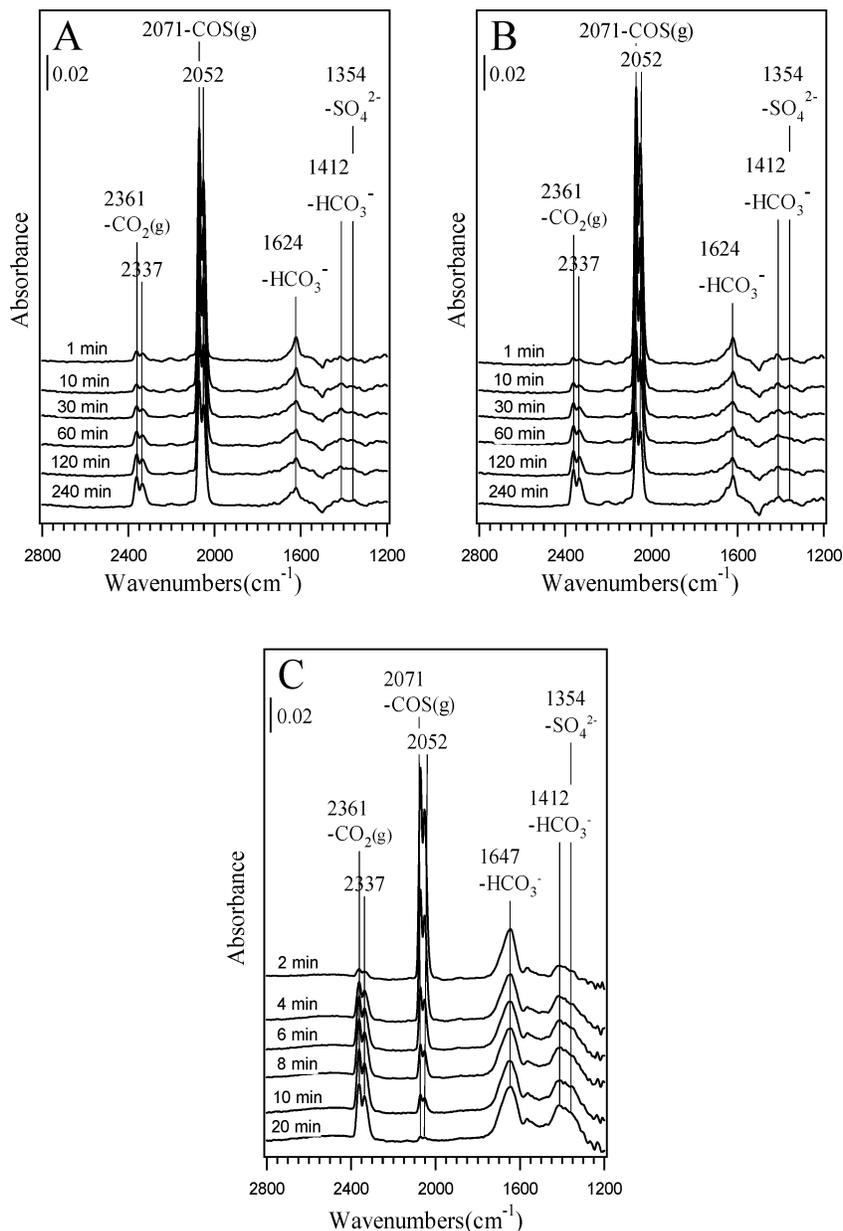
FIGURE 1. Dynamic changes of in situ DRIFTS spectra of the atmospheric particle sample (A), the preoxidized atmospheric particle sample (B), and the preoxidized Al_2O_3 sample (C) as a function of time after exposure to 500 ppm OCS + 95% O_2 in a closed system at 298 K.

spectra were collected and analyzed using a data acquisition computer installed with OMNIC 6.0 software (Nicolet Corp.). All spectra reported here were recorded at a resolution of 4 cm^{-1} for 100 scans.

2.3. Calibration Curve of Gas-Phase OCS Concentration. A series of in situ DRIFTS spectra at steady state of flow system with various concentrations of OCS (40–2000 ppm) were recorded at 298 K. The integrated areas of the absorption peak of gaseous OCS in the range of 1980–2120 cm^{-1} have a linear correlation with the concentration of OCS ($R^2 > 0.99$). On the basis of this result, the concentration of gas-phase OCS can be determined by measuring the in situ DRIFTS spectra peak areas of gaseous OCS.

3. Results and Discussion

3.1. Characterizations. *X-ray Fluorescence.* The inorganic elemental composition of the atmospheric particle sample was determined by XRF measurement. Table 1 exhibits that the major inorganic elements in the atmospheric particle sample are Si and Al, followed by Ca, S, Fe, and Mg.

TABLE 1. Inorganic Element Composition of the Atmospheric Particle Sample

element	Si	Al	Ca	S	Fe	Mg	K	Na	Ti	P
percent (%)	38.2	12.0	7.8	6.4	5.1	4.8	1.8	1.4	0.5	0.3

TABLE 2. Specific Area of the Atmospheric Particle Sample and the Al_2O_3 Sample

sample	atmospheric particles	Al_2O_3
BET area (m²/g)	4.8	277

BET. BET results are shown in Table 2. The Al_2O_3 sample has a much larger surface area than the atmospheric particle sample. Atmospheric particles and Al_2O_3 show a striking contrast for studying their catalytic reactivities and reaction mechanisms of OCS oxidation.

3.2. Heterogeneous Reaction of OCS on the Atmospheric Particle Sample, the Preoxidized Atmospheric Particle
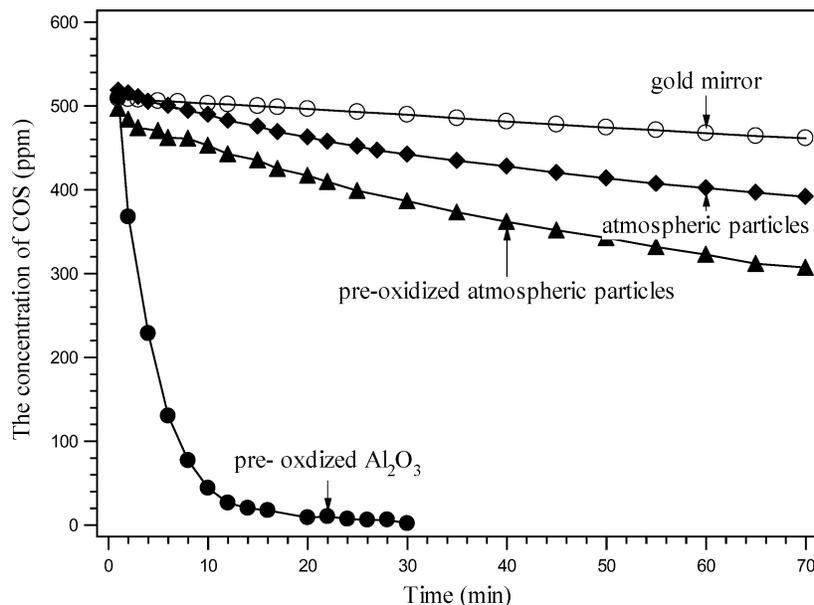
FIGURE 2. Heterogeneous reaction of 500 ppm OCS + 95% O₂ on the atmospheric particle sample, the preoxidized atmospheric particle sample, the preoxidized Al₂O₃ sample, or gold mirror at 298 K in a closed system.
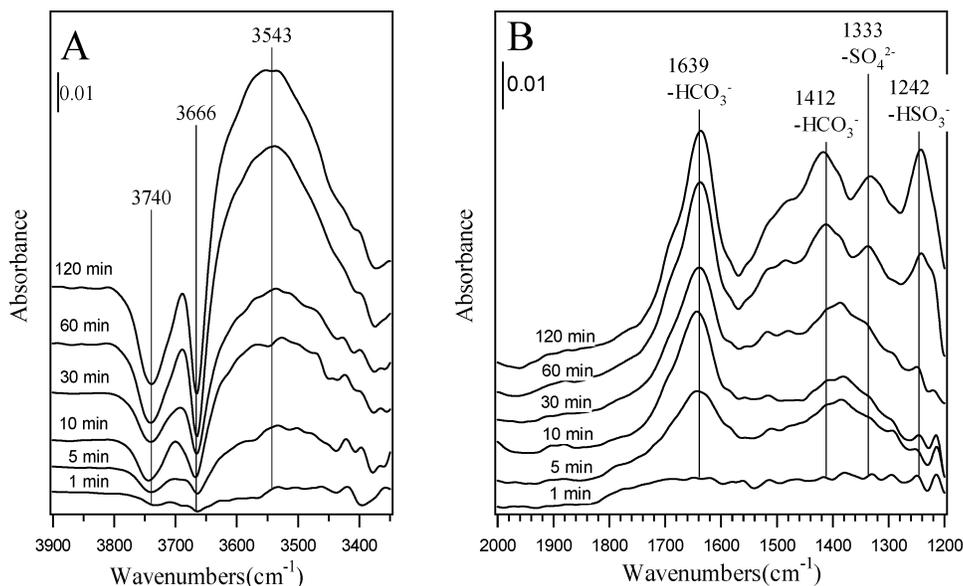
FIGURE 3. Dynamic changes of in situ DRIFTS spectra of the preoxidized Al₂O₃ sample as a function of time in a flow of 500 ppm OCS + 95% O₂ at 298 K.

Sample, and the Preoxidized Al₂O₃ Sample. The atmospheric particle sample was exposed to a flow of 500 ppm OCS + 95% O₂ at 298 K for 5 min, and then the inlet and outlet were closed. The in situ DRIFTS spectra on the atmospheric particle sample were recorded as a function of time as shown in Figure 1A. The same experiments were also carried out using the preoxidized atmospheric particle sample and the pre-oxidized Al₂O₃ sample. The results are shown in Figure 1B and C. In Figure 1A, B, and C strong peaks due to gas-phase OCS appeared at 2071 and 2052 cm⁻¹ (*13, 14*). A pair of peaks of gaseous carbon dioxide (CO_2) were observed at 2337 and 2361 cm⁻¹ (*15–17*). The bands at 1624 (1647), 1412 cm⁻¹ are due to surface HCO_3^- species (*13, 15–17*), and the band at 1354 cm⁻¹ is assigned to surface SO_4^{2-} species (*18–22*). It is also found that the peaks for gas-phase CO_2, surface HCO_3^-, and SO_4^{2-} species increase in intensity with time, while the peaks for gaseous OCS diminish, suggesting that OCS in O_2 can be converted into CO_2, surface HCO_3^-, and SO_4^{2-} species

on the samples of atmospheric particles, the preoxidized atmospheric particles, and the preoxidized Al₂O₃ at 298 K.

The gas-phase OCS concentration shown in Figure 2 was determined by comparing OCS absorbance peak area with the calibration curve of gas-phase OCS concentration. The control experiment with a gold mirror indicated that the system may consume a small quantity of OCS through the absorption or the heterogeneous reaction catalyzed by the surface of the system. The concentration of gaseous OCS decreases moderately with the atmospheric particle sample and the preoxidized atmospheric particle sample, whereas it decreases rapidly with the preoxidized Al₂O₃ sample. Since the final products over the atmospheric particle sample and the preoxidized Al₂O₃ sample are completely the same, this reaction rate is mostly determined by the surface area and catalytic activity. The preoxidized Al₂O₃ sample apparently has a larger surface area and higher catalytic activity than the atmospheric particle sample. Therefore, as a simplified
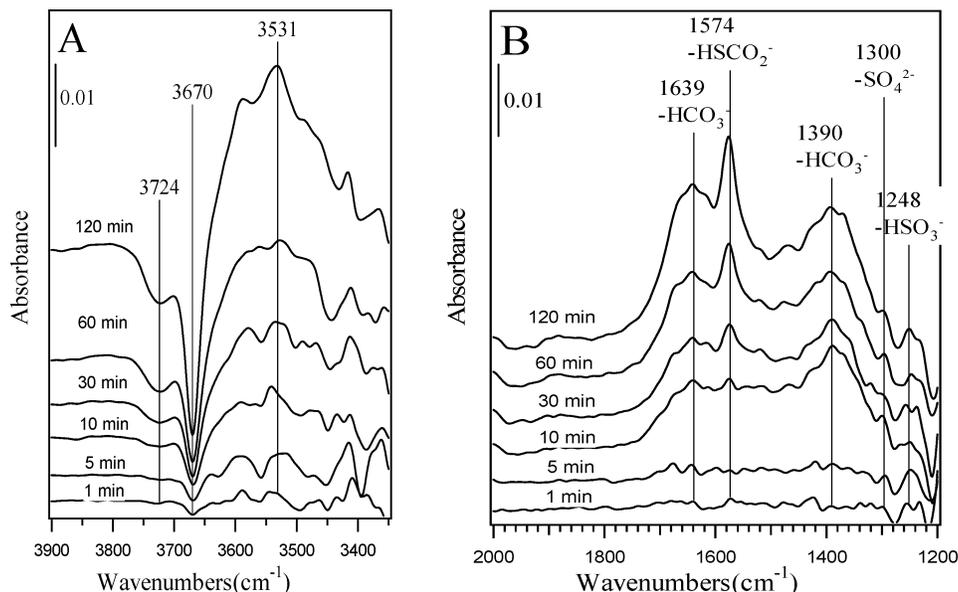
FIGURE 4. Dynamic changes of in situ DRIFTS spectra of the prereduced Al_2O_3 sample as a function of time in a flow of 500 ppm OCS + 95% H_2 at 298 K.
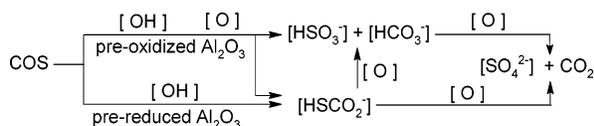
FIGURE 5. Mechanism of heterogeneous oxidation of OCS on the pretreated Al_2O_3 sample.

model, the reaction mechanism on the surface of Al_2O_3 was examined.

3.3. Dynamic State in Situ DRIFTS Study of OCS + 95% O_2 on the Preoxidized Al_2O_3 Sample in a Flow System. The preoxidized Al_2O_3 sample was exposed to a flow of 500 ppm OCS + 95% O_2 at 298 K. Figure 3 shows the in situ DRIFTS spectra of the preoxidized Al_2O_3 sample as a function of time in the system. It is evident that the intensities of the negative peaks at 3740 and 3666 cm^{-1} and the positive broad peak at 3543 cm^{-1} increased drastically with time (Figure 3A). In the model proposed by Peri (23, 24), these bands were attributed

to the vibrations of surface hydroxyl (OH) species. The band at 3543 cm^{-1} was assigned to the hydrogen binding of OCS or CO_2 or sulfur dioxide (SO_2) (19, 22). This result implies that the surface OH might be the reaction active site for OCS. Additionally, the peaks due to the adsorptions of surface SO_4^{2-} (1333 cm^{-1}), HCO_3^- (1639 and 1412 cm^{-1}), and HSO_3^- species (1242 cm^{-1}) were observed (25, 26), and the intensities of these peaks increased with time (Figure 3B).

To confirm our assignment about the surface SO_4^{2-} species, 1.0 g of preoxidized Al_2O_3 sample after exposure to a flow of 500 ppm OCS + 95% O_2 at 298 K for 2 h was analyzed by ion chromatography (DIONEX, CA); 2.43 mg/L SO_4^{2-} can be detected (sample stirred with 100 mL deionized water, and then filtered through a 0.45-μm filter). This result confirms the formation of the surface SO_4^{2-} species on the preoxidized Al_2O_3 sample.

3.4. Dynamic State in Situ DRIFTS Study of OCS + 95% H_2 on the Prereduced Al_2O_3 Sample in a Flow System. The above results confirm that OCS in O_2 can be heterogeneously
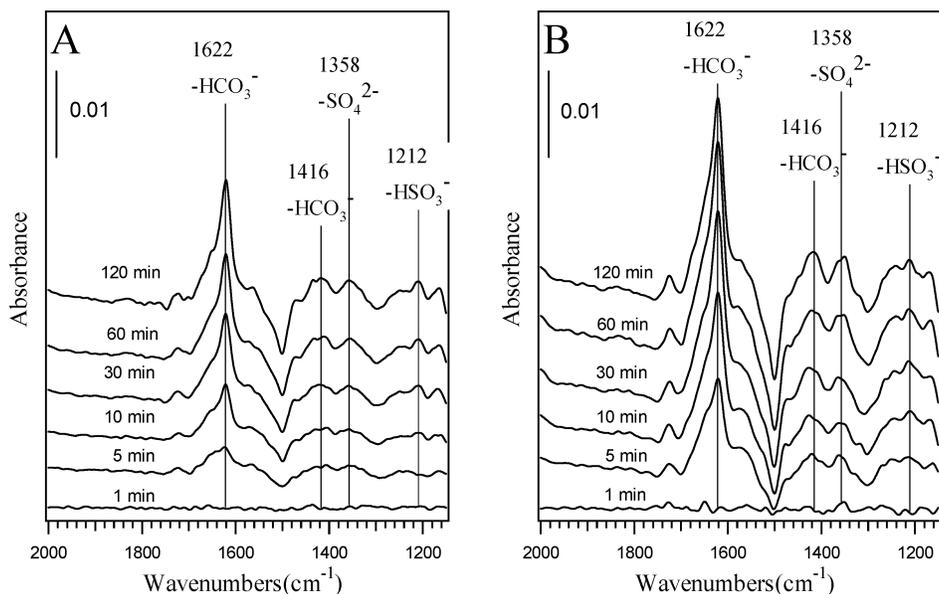
FIGURE 6. Dynamic changes of in situ DRIFTS spectra of the atmospheric particle sample (A) and the preoxidized atmospheric particle sample (B) as a function of time in a flow of 500 ppm OCS + 95% O_2 at 298 K.

oxidized into CO_2, surface HCO_3^-, and SO_4^{2-} species on the preoxidized Al_2O_3 sample. However, some other intermediates, key to the understanding of the mechanism of OCS conversion, were not identified in this rapid reaction. Considering that the H_2 pretreatment of Al_2O_3 is expected to weaken its catalytic activity for OCS oxidation, a further experiment was performed on the prereduced Al_2O_3 sample to characterize these intermediates.

Figure 4 shows the in situ DRIFTS spectra of the prereduced Al_2O_3 sample in a flow of 500 ppm OCS + 95% H_2 at 298 K. Compared with Figure 3, the 1639 and 1390 cm^{-1} bands indicated similar evidence for surface HCO_3^- species, but the bands associated with the surface SO_4^{2-} species at 1300 cm^{-1} and HSO_3^- species at 1248 cm^{-1} were significantly weak (Figure 4B). In contrast, a new peak at 1574 cm^{-1}, which was assigned to $HSCO_2^-$ (13, 27), was observed. It is apparent that the Al_2O_3 pretreated by H_2 slows down COS oxidation and enables the observation of a reaction intermediate. In the region of hydroxyl groups, a drastic increase in the intensity of negative peak attributed to the vibration of surface OH species at 3670 cm^{-1} was observed (Figure 4A). This strongly suggests that the formation of surface $HSCO_2^-$ species derives from the reaction between surface OH species and OCS. Comparing with Figure 3, pretreatment of Al_2O_3 using H_2 only reduces the formation of surface SO_4^{2-} and HSO_3^- species, but cannot block the formation of surface $HSCO_2^-$ and HCO_3^- species.

On the basis of the above results, we propose a mechanism of the heterogeneous oxidation of OCS on Al_2O_3 as shown in Figure 5.

OCS can be oxidized into CO_2, surface HSO_3^-, HCO_3^-, and SO_4^{2-} species on the preoxidized Al_2O_3 sample at room temperature. When active oxygen containing surface species was consumed, O_2 in the gas phase can supplement it so that the oxidation reaction can continue until the surface is covered by SO_4^{2-} species. While the prereduced Al_2O_3 sample is exposed to OCS + H_2, the reaction between surface OH and OCS occurs and further oxidation of OCS is slowed. As a result, surface $HSCO_2^-$ species became a dominant surface species under the reductive condition.

3.5. Dynamic State in Situ DRIFTS Study of OCS + 95% O_2 on the Atmospheric Particle Sample and the Preoxidized Atmospheric Particle Sample in a Flow System. Figure 6 shows the dynamic changes of the in situ DRIFTS spectra of the atmospheric particle sample (Figure 6A) and the preoxidized atmospheric particle sample (Figure 6B) exposed to a flow of 500 ppm OCS + 95% O_2 at 298 K as a function of time. In both Figure 6A and B, the surface SO_4^{2-} species (1358 cm^{-1}), HCO_3^- species (1622 and 1416 cm^{-1}), and HSO_3^- species (1212 cm^{-1}) were observed, and the intensity of these peaks increased with time. These results confirm that OCS can also be oxidized into CO_2, surface HSO_3^-, HCO_3^-, and SO_4^{2-} species on the atmospheric particle sample in a flow system at room temperature. Since the real atmospheric particle sample has relatively high surface area (4.8 m^2/g), its influence on the conversion of OCS in atmosphere is not neglectable. It should be noted that the preoxidized atmospheric particle sample shows a higher reactivity for its rich oxygen containing surface species. These results correspond with the proposed mechanism of the heterogeneous oxidation of OCS very well.

This study reveals that OCS can be catalytically oxidized on the real atmospheric particles and Al_2O_3 to produce gas-phase CO_2, surface HSO_3^-, HCO_3^-, and SO_4^{2-} species at room temperature. The pretreatment of Al_2O_3 obviously influenced the mechanism of OCS heterogeneous oxidation. The hydrogen thiocarbonate surface ($HSCO_2^-$) species, an intermediate formed in the reaction of OCS with surface hydroxyl (OH), can only be observed on the prereduced Al_2O_3 sample. The order of catalytic reactivity for heterogeneous oxidation of OCS is the preoxidized Al_2O_3 sample $\gg$ the preoxidized atmospheric particle sample > the atmospheric particle sample.

Literature Cited

(1) Torres, A. L.; Maroulis, P. J.; Goldberg, A. B.; Bandy, A. R. Atmospheric OCS measurements on project Gametag. *J. Geophys. Res.* **1980**, *85*, 7357−7360.

(2) Khalil, M. A. K.; Rasmussen, R. A. Global sources, lifetimes and mass balances of carbonyl sulfide (OCS) and carbon disulfide (CS_2) in the earth's atmosphere. *Atmos. Environ.* **1984**, *18*, 1805−1813.

(3) Andreae, M. O.; Crutzen, P. J. Atmospheric aerosols: biogeochemical sources and role in atmospheric chemistry. *Science* **1997**, *276*, 1052−1058.

(4) Crutzen, P. J. The possible importance of CSO for the sulfate layer of the stratosphere. *Geophys. Res. Lett.* **1976**, *3*, 73−76.

(5) Turco, R. P.; Whitten, R. C.; Toon, O. B.; Pollack, J. B.; Hamill, P. OCS, stratospheric aerosols and climate. *Nature* **1980**, *283*, 283−285.

(6) Watts, S. F. The mass budgets of carbonyl sulfide, dimethyl sulfide, carbon disulfide and hydrogen sulfide. *Atmos. Environ.* **2000**, *34*, 761−779.

(7) Baltensperger, U.; Ammann, M.; Kalberer, M.; Gäggeler, H. W. Chemical reactions on aerosol particle surfaces: concept and methods. *J. Aerosol Sci.* **1996**, *27*, S651−S652.

(8) Ravishankara, A. R. Heterogeneous and multiphase chemistry in the troposphere. *Science* **1997**, *276*, 1058−1065.

(9) Al-Abadleh, H. A.; Grassian, V. H. Oxide surfaces as environmental interfaces. *Surf. Sci. Rep.* **2003**, *52*, 63−161.

(10) Liu, C. L.; Chuang, T. T.; Dalla Lana, I. G. The oxidizing properties of γ-alumina: Infrared studies of the adsorption of H_2S and CS_2. *J. Catal.* **1972**, *26*, 474−476.

(11) Datta, A.; Cavell, R. G. Claus catalysis. 2. An FTIR study of the adsorption of H_2S on the alumina catalyst. *J. Phys. Chem.* **1985**, *89*, 450−454.

(12) Wang, L.; Zhang, F.; Chen, J. M. Carbonyl sulfide derived from catalytic oxidation of carbon disulfide over atmospheric particles. *Environ. Sci. Technol.* **2001**, *35*, 2543−2547.

(13) Lavalley, J. C.; Travert, J.; Chevreau, T.; Lamotte, J.; Saur, O. Infrared study of coadsorption of H_2S and CO_2 on γ-alumina. *J. Chem. Soc., Chem. Commun.* **1979**, *4*, 146−148.

(14) Dohrmann, J.; Glebov, A.; Toennies, J. P.; Weiss, H. Structure and dynamics of a monolayer OCS on NaCl (001): a combined FTIRS, HAS and LEED study. *Surf. Sci.* **1996**, *368*, 118−125.

(15) Amenomiya, Y.; Morikawa, Y.; Pleizier, G. Infrared spectroscopy of $C^{18}O_2$ on alumina. *J. Catal.* **1977**, *46*, 431−433.

(16) Morterra, C.; Zecchina, A.; Coluccia, S.; Chiorino, A. IR spectroscopic study of CO_2 adsorption onto η-Al_2O_3. *J. Chem. Soc., Faraday Trans.* ¢**1977**, *73*, 1544−1560.

(17) Nemeth, L.; Gati, G.; Gervasini, A.; Auroux, A.; Mink, G.; Pap, I. S.; Szekely, T. Kinetic study of the carbonyl sulphide synthesis from carbon dioxide and carbon disulphide on alumina catalysts. *Appl. Catal.* **1990**, *64*, 143−159.

(18) Saur, O.; Bensitel, M.; Mohammed Saad, A. B.; Lavalley, J. C.; Tripp, C. P.; Morrow, B. A. The structure and stability of sulfated alumina and titania. *J. Catal.* **1986**, *99*, 104−110.

(19) Lavalley, J. C. Infrared spectrometric studies of the surface basicity of metal oxides and zeolites using adsorbed probe molecules. *Catal. Today* **1996**, *27*, 377−401.

(20) Yang, R. T.; Li, W. B.; Chen, N. Reversible chemisorption of nitric oxide in the presence of oxygen on titania and titania modified with surface sulfate. *Appl. Catal., A* **1998**, *169*, 215−225.

(21) Meunier, F. C.; Ross, J. R. H. Effect of ex situ treatments with SO_2 on the activity of a low loading silver-alumina catalyst for the selective reduction of NO and NO_2 by propene. *Appl. Catal., B* **2000**, *24*, 23−32.

(22) Sahibed-Dine, A.; Aboulayt, A.; Bensitel, M.; Mohammed Saad, A. B.; Daturi, M.; Lavalley, J. C. IR study of CS_2 adsorption on metal oxides: relation with their surface oxygen basicity and mobility. *J. Mol. Catal. A: Chem.* **2000**, *162*, 125−134.

(23) Peri, J. B.; Hannan, R. B. Surface hydroxyl groups on γ-Alumina. *J. Phys. Chem.* **1960**, *64*, 1526−1530.

(24) Peri, J. B. A model for the surface of γ-alumina. *J. Phys. Chem.* **1965**, *69*, 220−230.

(25) Laniecki, M.; Ziólek, M.; Karge, H. G. Effect of water on the formation of HSO_3^- ions upon SO_2 adsorption onto Faujasite-type zeolites. *J. Phys. Chem.* **1987**, *91*, 4−6.

(26) Mitchell, M. B.; Sheinker, V. N.; White, M. G. Adsorption and reaction of sulfur dioxide on alumina and sodium-impregnated alumina. *J. Phys. Chem.* **1996**, *100*, 7550−7557.

(27) Hoggan, P. E.; Aboulayt, A.; Pieplu, A.; Nortier, P.; Lavalley, J. C. Mechanism of COS hydrolysis on alumina. *J. Catal.* **1994**, *149*, 300−306.